

# Quantitative WB-MRI with ADC histogram analysis for response assessment in diffuse bone disease

Danoob Dalili<sup>1</sup>; Anwar R. Padhani<sup>2</sup>; Robert Grimm<sup>3</sup>

<sup>1</sup> Imperial College Healthcare NHS Trust, St Mary's Hospital, London, United Kingdom

<sup>2</sup> Paul Strickland Scanner Centre, Mount Vernon Cancer Centre, Northwood, Middlesex, United Kingdom

<sup>3</sup> Siemens Healthineers, Erlangen, Germany

## Introduction

Tumor heterogeneity occurs at multiple levels with marked differences in cell mix, size and arrangements. Heterogeneity also exists in microenvironmental factors (including oxygenation, pH, interstitial pressure, blood flow), metabolism and gene expression. This profound heterogeneity is extremely important for prognosis, therapy planning, drug delivery, ultimately affecting patient outcomes. There are numerous ways of inves-

tigating tumor heterogeneity, which include using functional and molecular imaging, some of which can be applied to clinical data [1].

Quantitative assessment of tissue water diffusivity using ADC values allows tissue microstructure at a  $\mu\text{m}$ – $\text{mm}$  scale to be evaluated, thus reflecting tissue cellularity, organisation and blood flow. Most studies investigating

*Continued on page 61.*

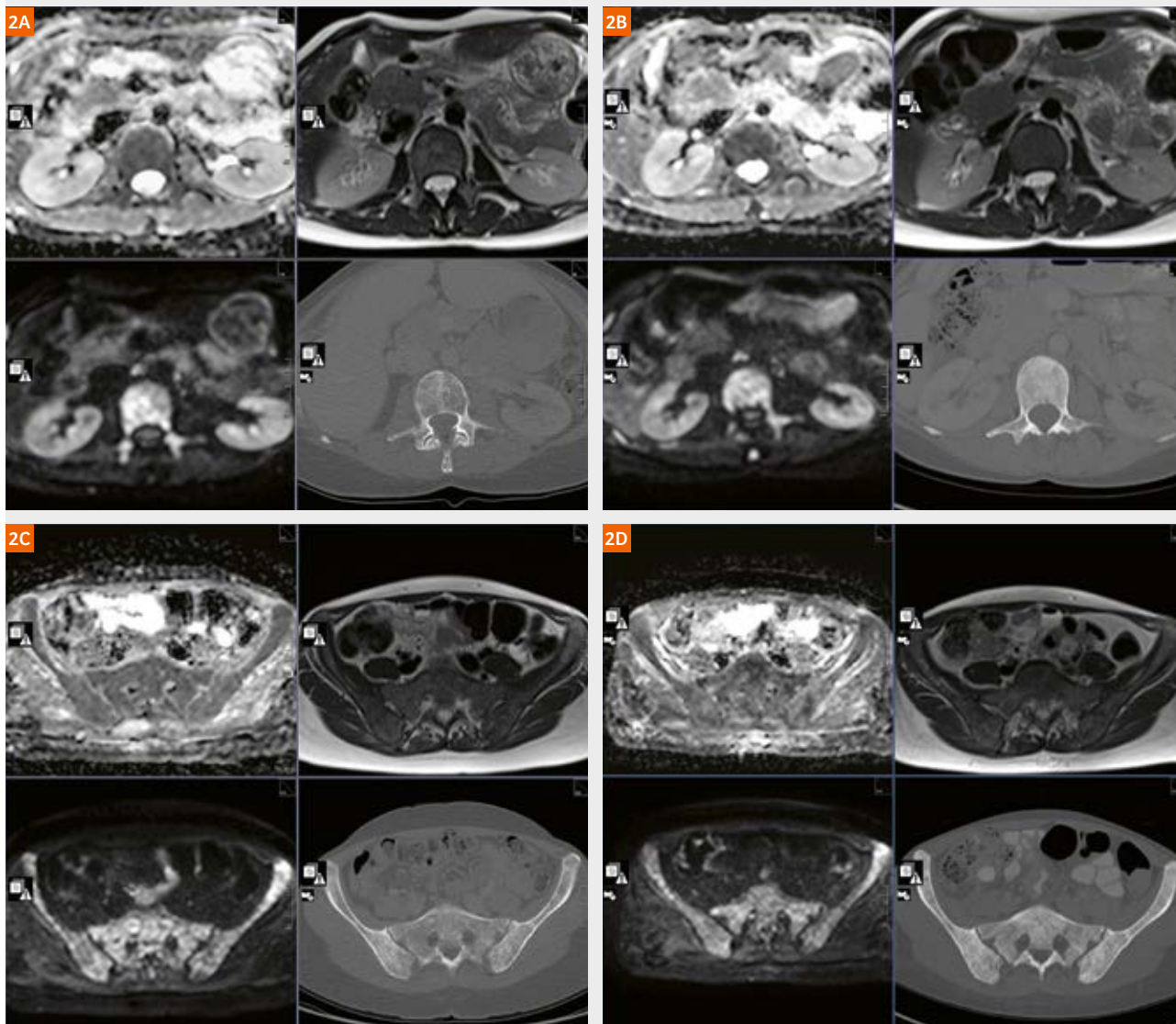
Figure 1: Morphological images and 3D DWI MIPs (inverted scale).



Left 2-columns: Whole-spine sagittal STIR sequences show diffuse bone marrow infiltration at baseline (1A) with no interval changes following hormonal therapy (1B). Middle 2-columns: Whole-spine sagittal T1-weighted images show diffuse bone marrow infiltration with no appreciable return of bone marrow fat after therapy (1D).

Right 2-columns: Whole-body b900 3D MIP (inverted scale). The bone marrow is diffusely involved with diffuse regions of high-signal intensity in the axial skeleton and in the proximal limb bones prior to therapy. A minor global reduction in the b900 signal intensity of bone marrow can be seen but this is not very convincing (1F).

Figure 2: Morphologic and diffusion-weighted axial sequences with axial bone window CT images of the L3 vertebral body and sacrum before and on hormonal therapy with bisphosphonates.

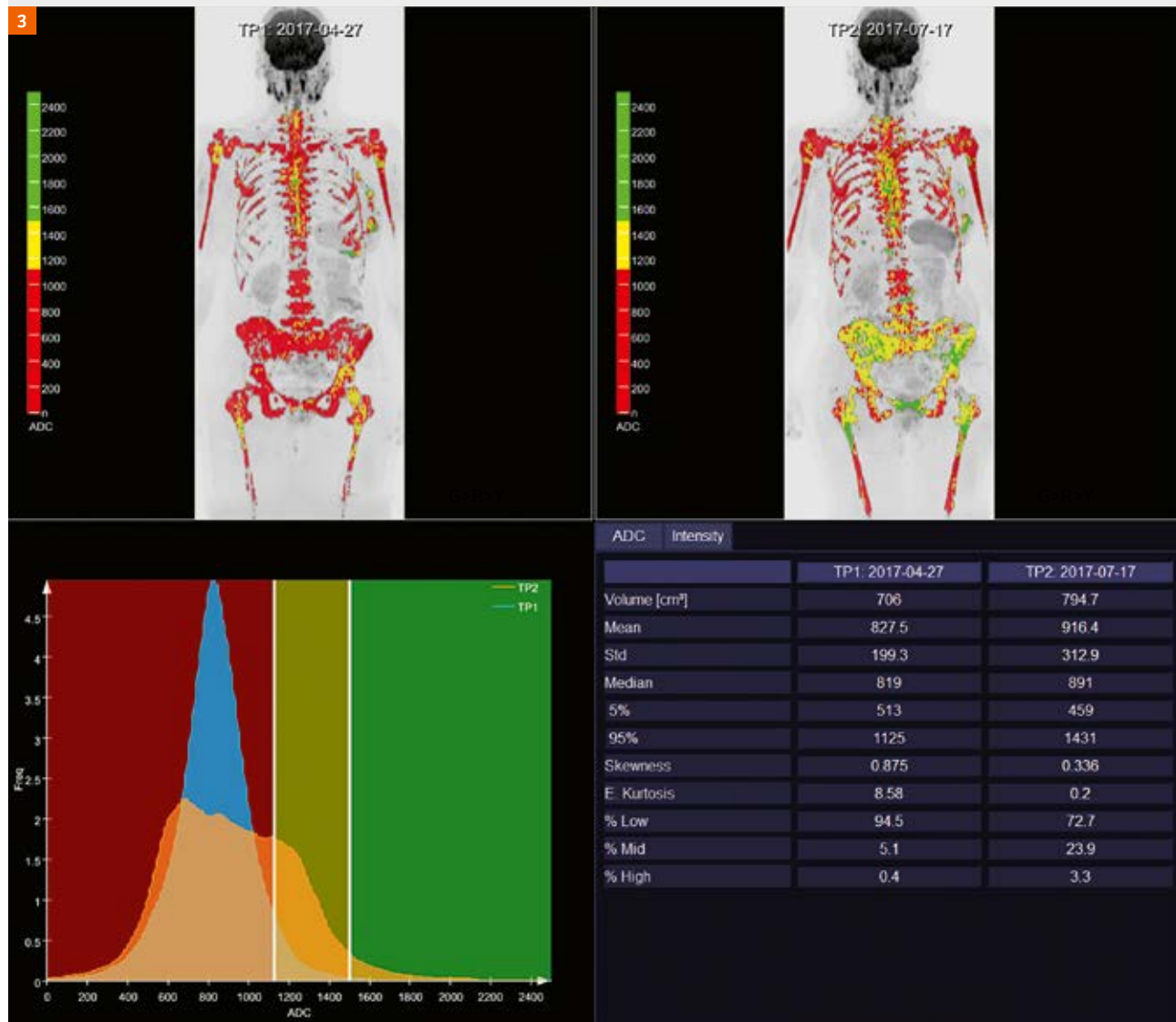


Axial ADC, T2w-HASTE, b900 and axial bone window CT scan images before and during therapy through the L3 vertebral body (2A, B) and sacrum (2C, D).

Figures 2A and 2B: the L3 vertebral body marrow shows no change in ADC values but there is some decrease in the b900 signal intensity. A uniform increase in CT density with 'milky appearance' of the bone is consistent with responding disease (CT density 300 HU before therapy and 550 HU after therapy). However, the persistent elevated signal intensity on the b900 images suggests the ongoing presence of active disease.

Figures 2C and 2D: the CT scan shows a uniform increase in bone density (CT density 315 HU before therapy and 530 HU after therapy). Again the CT density change is not high enough to be confident regarding response. However, the ADC maps show intermixing of high and low ADC value voxels resulting in a textural change.

Figure 3: Whole-body tumor load analysis.



WB-tumor load segmentations were undertaken on *syngo.via* Frontier MR Total Tumor Load software<sup>1</sup>. The whole-body b900 images were segmented using computed b-value images of 900–1000 s/mm<sup>2</sup>, setting a signal intensity threshold of 100 AU. Extraneous signals (such as the brain, kidneys, spleen and bowel) were removed, to leave only recognizable bone disease sites. The b900 MIP images are overlaid with ADC value classes using the 95<sup>th</sup> centile value of the pre-treatment histogram (1125  $\mu\text{m}^2/\text{s}$ ) and 1500  $\mu\text{m}^2/\text{s}$ .

Red colored voxels represent untreated disease or those with no-detectable response.

Green colored voxels have ADC values  $\geq 1500 \mu\text{m}^2/\text{s}$  (representing voxels that are 'highly likely' to be responding).

The yellow voxels lie between the 95<sup>th</sup> centile value of the pre-treatment histogram (1125  $\mu\text{m}^2/\text{s}$ ) and 1500  $\mu\text{m}^2/\text{s}$ . Thus, yellow voxels represent regions 'likely' to be responding.

706 mL of bone marrow was segmented before therapy and 795 mL after therapy. Note that there is no significant increase in median ADC values (819  $\mu\text{m}^2/\text{s}$  and 891  $\mu\text{m}^2/\text{s}$  respectively), but a decrease in excess kurtosis (8.6 and 0.2 respectively), and broadening of ADC histogram and an increase in the standard deviation (199 and 313  $\mu\text{m}^2/\text{s}$  respectively) can be seen on the corresponding relative frequency histograms. There is a unimodal distribution of ADC values at baseline (TP1) and a plateau distribution of the post-treatment (TP2) histogram.

The whole-body ADC color projections focusing on response (ADC maximum intensity projections) for both time points are shown. A spatial discordant response pattern is visible with responding increasing yellow and green voxels in the pelvis and proximal femora.

<sup>1</sup> *syngo.via* Frontier is for research only, not a medical device. *syngo.via* Frontier MR Total Tumor Load is a released research prototype.

the usefulness of diffusion imaging for disease characterization, prognostication and therapy response use region-of-interest (ROI) approaches deriving mean values of ADC (unit:  $\mu\text{m}^2/\text{s}$ ). This averaging method can be used to assess heterogeneity between ROIs or between patients, but fundamentally, ignores the heterogeneity within the ROI.

The characterization of tissues can be improved using histogram-based assessments of the distribution of ADC values. Histogram approaches have multiple advantages, including volume-of-interest (VOI) assessments, thus avoiding the subjectivity that is inherent with ROI placements. Importantly, histograms can provide additional metrics that reflect the texture of lesions, thereby allowing heterogeneity of ADC distribution within tissue to be assessed.

Histogram-based ADC analyses have mostly been undertaken in the context of neuroimaging showing added value for brain tumor grading, prognosis and therapy response [2–4]. However, this approach is increasing being applied to extracranial tissues, including evaluations of cervix and breast cancers [5–7], liver fibrosis [8], peritoneal malignancy [9] and bone metastases [10, 11]. These and other studies, have shown the potential of ADC histogram descriptors to improve the characterization of tissues, as well as to serve as prognostic and response biomarkers.

In this report, we describe a patient with breast cancer metastasising to the bone marrow, who underwent hormonal treatment. CT scans, morphologic MR images and ROI derived ADC assessments were confusing when trying to gauge the success of therapy. Volume based assessments of whole-body tumor load and ADC histograms, enabled an accurate assessment of the clinical status allowing therapy to be continued.

## Case study

A 37-year-old woman presenting with a 2-year history of lower back pain was found to have diffuse metastatic bone infiltration following an MRI of her lumbar spine. A bone marrow trephine biopsy and core biopsy of an asymptomatic left breast mass showed the presence of metastatic ER-positive, HER2 2+ (FISH-negative), grade 2 invasive ductal carcinoma of the breast. She was commenced on systemic anticancer hormonal therapy with Tamoxifen and Goserelin as well as with Zoledronic acid infusions.

She underwent baseline and 3 month follow-up whole-body MRI scans with diffusion-weighted sequences using a 1.5T MAGNETOM Avanto scanner using a published protocol [12]. The baseline scan demonstrated extensive metastatic bone only disease (Figs. 1, 2) that does not change appreciably on morphological T1w, T2w and

STIR images of the spine. CT scans undertaken at the corresponding time points, show uniform increases in bone density with a ‘milky texture’ which are difficult to interpret regarding the activity of the underlying disease. It’s only when CT density increases to  $>850$  HU that it is possible to be confident about the likelihood of inactive disease [13]. There was minimal reduction in b900 signal intensity.

The diffusion-weighted images for both timepoints were analysed using the threshold-based segmentation, *syngo.via* Frontier MR Total Tumor Load software<sup>1</sup> [14]. The pre-treatment ADC histogram has a unimodal distribution of ADC values with high excess kurtosis (Fig. 3). After 3 months of hormonal therapy, a plateau distribution of ADC values can be seen with little change in the mean ADC but a greater spread in ADC values can be appreciated. Responding voxels (yellow/green voxels) are mostly seen in the pelvis and proximal femora on the ADC color projections focusing on response. These ADC histograms are consistent with a favorable therapy response, because of which treatment was continued.

## Discussion

There are a variety of approaches for objectively displaying and analyzing ADC images in response assessment settings. Most studies report mean values from single/multiple ROIs placed on high b-value images, which are then copied on ADC maps for quantitate ADC value readouts. Recently, studies have begun to report on central tendency measures (mean, median, mode values) of ADC histograms on volumes of interest (VOIs). Because bone metastases are heterogeneous in their spatial ADC distributions, these simpler, first order measures have limited abilities to detect treatment-related changes, particularly if there are both increases and decreases in ADC in response to treatment (for example, when ADC values increase due to tumor cell kill and decrease due to bone marrow renormalization, fibrosis and dehydration) [15]. As a result, the net mean/median ADC change may be minimal. Furthermore, if large cystic or necrotic areas are present, then the ability to detect therapy response induced changes may be blunted.

More complex changes in ADC values can be evaluated by assessing the spread of the ADC data (variance, standard deviation, range (maximum–minimum difference), centile ranges, histogram entropy). The spread of ADC data allows estimates of the proportions of responding or non-responding tumor volume to be determined by the application of threshold cut-off values. So, in this case,

<sup>1</sup> *syngo.via* Frontier is for research only, not a medical device.  
*syngo.via* Frontier MR Total Tumor Load is a released research prototype.

the proportion of voxels in the active range (ADC-low voxels below  $1125 \mu\text{m}^2/\text{s}$ ) is 95% and 73% respectively at the two time-points.

Other higher order descriptors of histograms such as skewness (a measure of the degree of asymmetry of a distribution) and kurtosis (which is the degree of peakedness of a distribution) can also be helpful for evaluating therapy response. Comparison of relative frequency histograms to normal distributions allows quantitative values to be assigned to histogram kurtosis; positive excess kurtosis values  $>0$  (leptokurtic shape) indicates a higher peak than for a normal distribution (normal distribution shape is described as mesokurtic with an excess kurtosis value = 0). After therapy, excess kurtosis decreases often reaching values  $<0$  (platykurtic).

Readers should also be aware that both measurement (e.g. poor SNR) and analysis methods (e.g., two-point fitting for generating ADC values) can alter the skewness of histograms independent of therapy induced effects, because of which the quality of ADC maps images should be critically assessed, before higher order histogram descriptors such as maximum and minimum values, range and skewness are used to infer biologic significance.

#### ADC histogram analysis for assessing bone metastases

ADC histograms of untreated bone metastases are often positively skewed (tail to the right) with positive excess kurtosis. For our data acquisition protocol that uses b50, b600 and b900  $\text{mm}^2/\text{s}$  diffusion-sensitizing gradients, the majority of tumor ADC pixel values usually lie in the 650–1500  $\mu\text{m}^2/\text{s}$  range for untreated disease. Positive excess kurtosis is often maintained in the setting of tumor progression or in stable disease, although mean/median values may change depending on the relative extent of tumor infiltration and fat content in the bone marrow. If tumors are necrotic before treatment or if there has been a response to prior treatments, then more complex histogram shapes can be seen.

When tumors respond successfully to therapy, kurtosis values generally decrease and the standard deviation/variance increases. Negative skewness (tail to the left) often develops if the histogram retains a unimodal shape. Thus, the transformation of a positive kurtosis, positively skewed unimodal ADC distribution into a plateau shape in response to a therapy indicates likely response even in the absence of a significant change in mean/median ADC values. Where successful response is accompanied by regeneration of the normal bone marrow as part of the healing process, a distinct second ADC peak below the tumor peak can be observed which is illustrated in two accompanying cases within this issue of MAGNETOM Flash [15, 16].

Radiologists often enquire when there is an absolute need to use ADC histograms in “daily clinical practice”? Generally, we find ADC analyses are most useful in the presence of extensive, diffuse metastatic disease on WB-DWI or when there has been an apparent mixed/heterogeneous response to therapy. In these patients, visual inspections of morphological and diffusion-weighted images can be problematic and applying the MET-RADS response criteria [12] can be challenging due to the high volume of disease present. In these cases, we find histogram analyses indispensable because of the ability to observe changes in the spread, skewness and kurtosis of the ADC data.

#### References

1. Just N. Improving tumour heterogeneity MRI assessment with histograms. *British journal of cancer*. 2014 Dec 9;111(12):2205-13.
2. Song YS, Choi SH, Park CK, Yi KS, Lee WJ, Yun TJ, Kim TM, Lee SH, Kim JH, Sohn CH, Park SH. True progression versus pseudoprogression in the treatment of glioblastomas: a comparison study of normalized cerebral blood volume and apparent diffusion coefficient by histogram analysis. *Korean journal of radiology*. 2013 Aug 1;14(4):662-72.
3. Gutierrez DR, Awwad A, Meijer L, Manita M, Jaspan T, Dineen RA, Grundy RG, Auer DP. Metrics and textural features of MRI diffusion to improve classification of pediatric posterior fossa tumors. *American Journal of Neuroradiology*. 2014 May 1;35(5):1009-15.
4. Tozer DJ, Jäger HR, Dancheviji N, Benton CE, Tofts PS, Rees JH, Waldman AD. Apparent diffusion coefficient histograms may predict low grade glioma subtype. *NMR in biomedicine*. 2007 Feb 1;20(1):49-57.
5. Rosenkrantz AB. Histogram-based apparent diffusion coefficient analysis: an emerging tool for cervical cancer characterization?. *American Journal of Roentgenology*. 2013 Feb;200(2):311-3.
6. Downey K, Riches SF, Morgan VA, Giles SL, Attygalle AD, Ind TE, Barton DP, Shepherd JH, deSouza NM. Relationship between imaging biomarkers of stage I cervical cancer and poor-prognosis histologic features: quantitative histogram analysis of diffusion-weighted MR images. *American Journal of Roentgenology*. 2013 Feb;200(2):314-20.
7. Johansen R, Jensen LR, Rydland J, Goa PE, Kvistad KA, Bathen TF, Axelsson DE, Lundgren S, Gribbestad IS. Predicting survival and early clinical response to primary chemotherapy for patients with locally advanced breast cancer using DCE MRI. *Journal of Magnetic Resonance Imaging*. 2009 Jun 1;29(6):1300-7.
8. Fujimoto K, Tonan T, Azuma S, Kage M, Nakashima O, Johkoh T, Hayabuchi N, Okuda K, Kawaguchi T, Sata M, Qayyum A. Evaluation of the mean and entropy of apparent diffusion coefficient values in chronic hepatitis C: correlation with pathologic fibrosis stage and inflammatory activity grade. *Radiology*. 2011 Mar;258(3):739-48.
9. Kyriazi S, Collins DJ, Messiou C, Pennert K, Davidson RL, Giles SL, Kaye SB, deSouza NM. Metastatic ovarian and primary peritoneal cancer: assessing chemotherapy response with diffusion-weighted MR imaging—value of histogram analysis of apparent diffusion coefficients. *Radiology*. 2011 Oct;261(1):182-92.
10. Blackledge MD, Collins DJ, Tunariu N, Orton MR, Padhani AR, Leach MO, Koh DM. Assessment of treatment response by total tumor volume and global apparent diffusion coefficient using diffusion-weighted MRI in patients with metastatic bone disease: a feasibility study. *PLoS One*. 2014 Apr 7;9(4):e91779.

11. Perez-Lopez R, Mateo J, Mossop H, Blackledge MD, Collins DJ, Rata M, Morgan VA, Macdonald A, Sandhu S, Lorente D, Rescigno P. Diffusion-weighted imaging as a treatment response biomarker for evaluating bone metastases in prostate cancer: a pilot study. *Radiology*. 2016 Nov 22;283(1):168-77.
12. Padhani AR, Lecouvet FE, Tunariu N, Koh DM, De Keyzer F, Collins DJ, Sala E, Schlemmer HP, Petralia G, Vargas HA, Fanti S. METastasis Reporting and Data System for Prostate Cancer: practical guidelines for acquisition, interpretation, and reporting of whole-body magnetic resonance imaging-based evaluations of multiorgan involvement in advanced prostate cancer. *European urology*. 2017 Jan 31;71(1):81-92.
13. Beheshti M, Vali R, Waldenberger P, Fitz F, Nader M, Hammer J, Loidl W, Pirich C, Fogelman I, Langsteger W. The use of F-18 choline PET in the assessment of bone metastases in prostate cancer: correlation with morphological changes on CT. *Molecular imaging and biology*. 2010 Feb 1;12(1):98-107.
14. Grimm R, Padhani AR. Whole-body Diffusion-weighted MR Image Analysis with *syngo.via* Frontier MR Total Tumor Load. *MAGNETOM Flash* (68) 2/2017, 73-75.
15. Dalili D, Joshi P, Grimm R, Padhani AR. Evolution of the malignant bone marrow with successful therapy – quantitative analysis with whole body diffusion MRI. *MAGNETOM Flash* (69) 3/2017, 47–52.
16. Dalili D, Padhani AR, Grimm R. Quantitative WB-MRI with ADC histogram analysis for demonstrating complex response of bone marrow metastatic disease. *MAGNETOM Flash* 2017; 69(3): 38–42.



**Contact**

Dr. Danoob Dalili  
 Specialist Registrar Clinical Radiology  
 Imperial College Healthcare NHS Trust  
 St Mary's Hospital  
 Praed St  
 London W2 1NY  
 United Kingdom  
 Phone: +44 (0) 20 3312 6666  
 Dalili@doctors.org.uk



Prof. Anwar R. Padhani  
 Consultant Radiologist and  
 Professor of Cancer Imaging  
 Paul Strickland Scanner Centre  
 Mount Vernon Cancer Centre  
 Rickmansworth Road  
 Northwood, Middlesex HA6 2RN  
 United Kingdom  
 Phone (PA): +44-(0) 1923-844751  
 Fax: +44-(0) 1923-844600  
 anwar.padhani@stricklandscanner.org.uk

## Whole-body MRI at 1.5T – a How-to Guide, .exar1 protocol file and a video

Whole-body MRI has been used at Paul Strickland Scanner Centre (Northwood, UK) for over 10 years. In that time over 4000 examinations have been performed using a protocol designed to enable the detection and surveillance of metastatic bone and soft tissue disease.

Will McGuire, Deputy Superintendent MRI Radiographer, shares his protocol along with a video demonstrating the use of this protocol.



Visit [www.siemens.com/wb-mri](http://www.siemens.com/wb-mri) to download the material.

